Classical Electrostatics in Biology and Chemistry

Barry Honig; Anthony Nicholls

Science, New Series, Vol. 268, No. 5214. (May 26, 1995), pp. 1144-1149.

Stable URL:

http://links.jstor.org/sici?sici=0036-8075%2819950526%293%3A268%3A5214%3C1144%3ACEIBAC%3E2.0.CO%3B2-X

Science is currently published by American Association for the Advancement of Science.

Classical Electrostatics in Biology and Chemistry

Barry Honig* and Anthony Nicholls

A major revival in the use of classical electrostatics as an approach to the study of charged and polar molecules in aqueous solution has been made possible through the development of fast numerical and computational methods to solve the Poisson-Boltzmann equation for solute molecules that have complex shapes and charge distributions. Graphical visualization of the calculated electrostatic potentials generated by proteins and nucleic acids has revealed insights into the role of electrostatic interactions in a wide range of biological phenomena. Classical electrostatics has also proved to be a successful quantitative tool yielding accurate descriptions of electrical potentials, diffusion limited processes, pH-dependent properties of proteins, ionic strength–dependent phenomena, and the solvation free energies of organic molecules.

Electrostatic interactions play a central role in a variety of biological processes. A detailed characterization of the strength and nature of these interactions requires an understanding of the physical chemical properties of molecules in aqueous solution. Although the principles underlying solvent effects on solute properties have been understood for many years, methods that translate these principles into accurate predictions of experimental observables were generally not available. In the past few years, there have been significant advances in this direction, motivated primarily by problems of major biological as well as practical importance such as structure-based drug design and protein folding.

Understanding the properties of aqueous solutions requires models of the solute, the solvent, and the interactions between them. In the widely used molecular mechanics approach, solute or solvent molecules or both are described in terms of a "force field" where nonbonded van der Waals and electrostatic terms account for most of the details of intermolecular interactions. A proper description at the molecular level of solvent effects requires the calculation of the mutual interactions of a large number of molecules and the averaging of these over many solvent configurations. The daunting computational requirements of this approach have been partly overcome through theoretical advances and by continuing enhancements in computational power. Nevertheless, for many applications, the explicit treatment of solvent molecules and mobile ions is not feasible.

An alternative approach involves continuum or macroscopic models, in which solvent properties are described in terms of average values. Continuum methods were widely used in the past but fell into disfavor with the advent of modern simulation techniques. However, macroscopic solvent models have experienced a resurgence in recent years, partly because of computational and algorithmic advances that have made it possible to describe solute molecules in atomic detail while treating only the solvent in terms of average properties. In particular, the importance of classical electrostatics as providing an important qualitative paradigm and quantitative tool in structural biology, biochemistry, and chemistry has been widely recognized.

The Poisson-Boltzmann Equation

The classical treatment of electrostatic interactions in solution is based on the Poisson-Boltzmann equation (PBE)

$$\nabla \cdot [\varepsilon(\mathbf{r})\nabla \cdot \phi(\mathbf{r})] - \varepsilon(\mathbf{r})\kappa(\mathbf{r})^2 \sinh[\phi(\mathbf{r})]$$
$$+ 4\pi\rho^f(\mathbf{r})/kT = 0 \qquad (1)$$

where $\phi(\mathbf{r})$ is the dimensionless electrostatic potential in units of kT/q (k is the Boltzmann constant, T is the absolute temperature, and q is the charge on a proton), ε is the dielectric constant, and ρ^f is the fixed charge density (in proton charge units). The term $\kappa^2 = 1/\lambda^2 = 8\pi q^2 I/ekT$, where λ is the Debye length and I is the ionic strength of the bulk solution. The variables ϕ, ε, κ, and ρ are all functions of the position vector $\mathbf{r}$.

The second term of Eq. 1 accounts for salt effects and is absent when no mobile ions are present in the system ($\kappa = 0$). Under this condition, Eq. 1 reduces to Poisson's equation, which in turn reduces to Coulomb's law when the dielectric constant is uniform throughout space. However, because water is much more easily polarized by an electric field than are most solutes, at least two ε's are required to capture the underlying physics of polar molecules in aqueous solution. The effect of having two dielectric constants is expressed in Eq. 1 through the derivative of $\varepsilon(\mathbf{r})$ in the first term, which is nonzero only where $\varepsilon(\mathbf{r})$ varies. In all of the applications considered below, this region corresponds to the molecular surface, where there is a dielectric "discontinuity" between the low-ε solute and the high-ε solvent.

An intuitive understanding of the effect of the shape of the solute-solvent interface can be obtained from the concept of induced surface charge. Poisson's equation can be recast with a single dielectric model (Coulomb's law), where charge of polarity opposite to that of $\phi(\mathbf{r})$ is induced at the molecular surface. An important example is the simple case of a positive charge at the center of a low-ε sphere, which induces a negative charge distributed over the surface of the sphere. The positive potential in the solvent caused by the fixed positive charge will be screened by the negative surface charge; the higher the solvent's value of ε, the greater the surface charge, and hence, the greater the screening. Similarly, the favorable interaction of the fixed positive charge with its induced negative surface charge (which produces a "reaction field") is the basis of continuum solvation models. It is tempting to think of the induced surface charge as corresponding to an alignment of water dipoles at the molecular surface producing an excess local charge, and indeed, this is part of the effect. However, it should be realized that the surface charge description accounts for the polarization of the entire solvent.

The treatment of molecules in solution used here follows the general treatment developed by Born (1), Kirkwood (2), and Onsager (3) in which a solute molecule is described as a low-ε "cavity" embedded in a medium with a different value of ε. Because analytical solutions to Poisson's equation are only available for simple geometric objects, all applications of the PBE to molecules in solution, until recently, required a simplifying assumption for the shape of the solute and its charge distribution. For example, small solutes and proteins were treated as spheres, DNA as cylinders, and membranes as planes. However, numerical solutions to the PBE now make it possible to describe the shape of the solute in atomic detail while retaining a simplified "continuum" description of only the solvent.

Although the discussion so far has focused on Poisson's equation, many of the same concepts are applicable to the PBE as

The authors are in the Department of Biochemistry and Molecular Biophysics, Columbia University, New York, NY 10032, USA.

*To whom correspondence should be addressed.

well. Under conditions where $\phi(r)$ is small relative to kT, the sinh term can be linearized by setting $\sinh(\phi) = \phi$, yielding the linearized PBE (which reduces to Debye-Huckel theory when no dielectric discontinuity is present). In the linearized PBE, the ion atmosphere behaves much like the high-ϵ solvent in that both respond linearly to the electrical potential induced by fixed charges. In cases where the nonlinear PBE must be applied [for example, the ion atmosphere around highly charged macromolecules such as DNA or polylysine (4)], some of the simplicity of linear response theory is lost.

Calculating Electrical Potentials

The molecular surface is defined as the contact surface formed between the van der Waals envelope of the molecule and a probe solvent molecule (5). All regions inside the surface are assigned a low value of ϵ [~2 to 4 (6)], whereas exterior regions are assigned the ϵ of water (~80). The charge distribution of the molecule is usually represented in the form of point charges located at atomic nuclei.

Numerical procedures to solve the PBE first require a discretization of some sort, for example, finite difference methods that map variables onto a grid. A number of analytical and numerical techniques have been reported that can describe molecular surfaces, even for complex molecules such as proteins, in a few seconds of computer time [CPU (central processing unit) time] on standard processors (7).

The second step usually involves an iterative procedure, where an initial guess to a solution is refined successively. Warwicker and Watson reported the first numerical (finite difference) solution to the Poisson equation for a protein (8). This result was followed by finite difference solutions to the full linear (9, 10) and nonlinear PBEs (11). In recent years, a variety of numerical methods have yielded increasingly faster and more accurate algorithms based on grid-based (12, 13), boundary element (14), and finite element methods (15). A standard workstation can now be used to calculate $\phi(r)$ for a molecule in a solution of arbitrary ionic strength in seconds to minutes of CPU time, depending on the size of the molecule and the level of accuracy required in a particular application.

Patterns of $\phi(r)$ in Proteins

Perhaps the most extensive application of continuum electrostatics in structural biology has been the visual representation of $\phi(r)$ for proteins. [The plots of $\phi(r)$ in this article are calculated with the DelPhi pro-
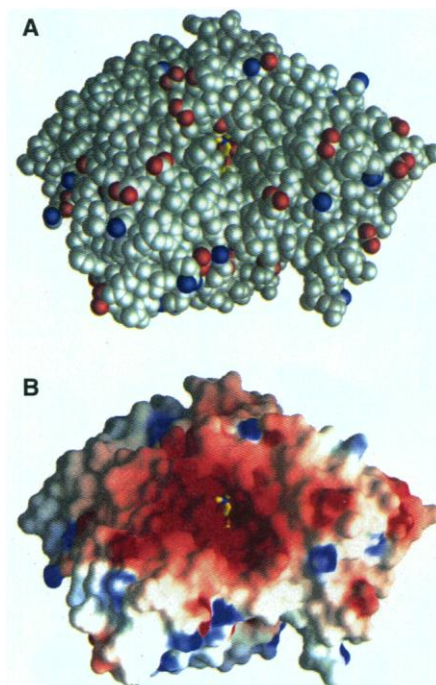
gram (12, 16) and displayed with GRASP (17).] Unexpectedly, proteins generate unique $\phi(r)$ patterns that, in many cases, have an important functional role. In addition to the specific location of charged and polar groups on the protein, the geometric shape of the molecular surface plays a crucial role in determining the form of the $\phi(r)$. The effect of shape arises through the existence of a boundary between the low-ϵ and high-ϵ regions.

Numerical solutions to the PBE equation yield information not evident from the three-dimensional (3D) structure alone. A hard-sphere representation of acetylcholinesterase (Fig. 1A) (18) shows a preponderance of negative charges on the face of the protein that borders the active site. However, the existence of an intense electronegative region centered in the active site (Fig. 1B) is not evident from the charge distribution in Fig. 1A. The pattern is due in large part to the depth of the active site pocket, which produces a dielectric dis-
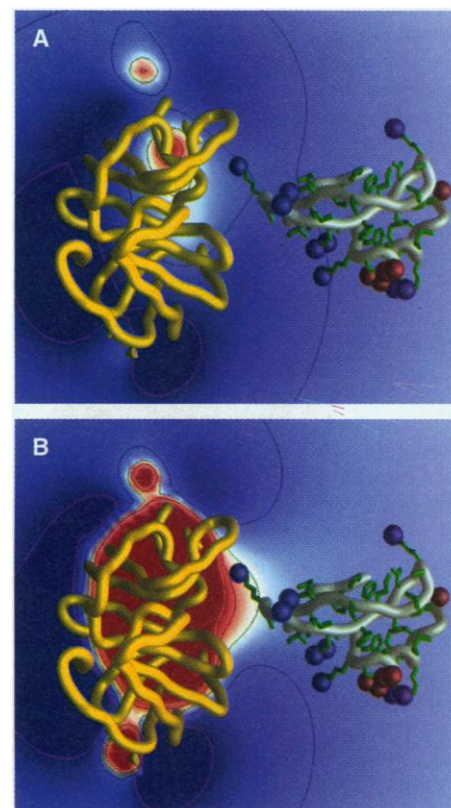

Fig. 1. Surface representations of acetylcholine esterase. (**A**) Space filling model (18). Atoms colored red are the oxygens of negatively charged carboxylate groups, and those colored blue are the nitrogens of positively charged basic groups. The substrate acetylcholine, which carries a net positive charge, is shown in yellow in the bottom of the active site. (**B**) Surface potential, displayed with GRASP (17). The molecular surface is color coded by electrostatic potential, as calculated with DelPhi (12) for the charges illustrated in (A). Potentials less than $-10kT$ are red, those greater than $10kT$ are blue, and neutral potentials (0 kT) are white. Linear interpolation was used to produce the color for surface potentials between these values. The active site is clearly distinguishable as a region of intense negative potential.

continuity with a distinctive shape.

The effect of the dielectric discontinuity is evident in Fig. 2, A and B, which illustrates the $\phi(r)$'s involved in the formation of the trypsin-trypsin inhibitor complex (19). Although both molecules have a large positive net charge, they form a very tight intermolecular complex. Whereas $\phi(r)$ for trypsin with a single ϵ throughout space (Fig. 2A) would suggest that bovine pancreatic trypsin inhibitor (BPTI) must dock into an area of large positive potential (which is highly unlikely given its own positive charge), a two-ϵ model (Fig. 2B) produces a significant local domain of negative potential at the binding site.

Reports of protein structures often include color-coded pictures representing so-

Fig. 2. Electrostatic potentials characteristic of the trypsin–bovine pancreatic trypsin inhibitor (BPTI) complex. Secondary structure representations for trypsin (left) and BPTI (right). The complex (49) has, for clarity, been partially separated along the axis of interaction (horizontal and parallel to the page). Also shown for BPTI are the positions of the charged atoms for ionizable side chains, color coded as in Fig. 1A. The $\phi(r)$'s were calculated for the charged groups of trypsin alone and are illustrated by a color-coded plane that slices through the binding site. The color code is the same as in Fig. 1B but with extrema of $\pm 2kT$. Contour lines are shown at -2, -1, 0, 1, and 2 kT (white, blue, green, red, and magenta, respectively) for potentials in this plane. The $\phi(r)$'s were calculated (**A**) assuming a uniform dielectric constant of 80 throughout space and (**B**) assuming an interior dielectric constant of 2 for trypsin and 80 elsewhere.

lutions to the PBE. An important finding that appears to be emerging from these studies is that many intermolecular interactions involve associations between surfaces with complementary $\phi(r)$'s. For example, DNA binding proteins generally have regions of positive $\phi(r)$ at the DNA binding interface (20). An example is shown in Fig. 3A, which displays $\phi(r)$ at the surface of the processivity factor of *Escherichia coli* DNA polymerase III (21). This protein forms a "sliding clamp" that binds tightly but non-specifically to DNA. The protein has a large negative net charge (-22 per dimer) but nevertheless displays a significant positive $\phi(r)$ on the inner DNA binding surface.

A neutral surface can also be functionally significant and is suggestive of hydrophobic interactions. Waksman *et al.* (22), in analyzing their structure of the Src SH2 domain in complexed and peptide-free forms, noticed that the binding site consisted of a neutral hydrophobic pocket, which binds isoleucine, and a region of positive $\phi(r)$, which binds phosphotyrosine (Fig. 3B). A striking example of a functionally significant zero potential region is provided by the F1 adenosine triphosphatase (ATPase) (23). The inner surfaces of its trimeric "wheel" and monomeric "stalk" are essentially neutral, providing a nonspecific, "greasy" axle for monomer rotation during ATP synthesis. In this system, the absence of charge in the interface may be essential because it would be energetically implausible for rotations to occur if buried ion-pairs were broken in the process.

Common electrostatic features within a family of related proteins can be identified by "electrostatic homology modeling," in which the primary focus is on the $\phi(r)$ patterns rather than on specific residues or 3D structure similarities. One example is provided by secretory phospholipases A$_2$, which have common asymmetries in their $\phi(r)$'s that appear to correlate with their preferential binding to negatively charged lipids (24). In another example, neurotrophic factors that share the same low-affinity receptor as nerve growth factor (NGF) appear to have a remarkably similar positive patch at the putative binding site (25). Finally, in comparing eukaryotic and bacterial DNA polymerase processivity factors, Krishna *et al.* (26) found a highly similar $\phi(r)$ pattern even though the two proteins have very low subunit sequence homology (15%). Moreover, the eukaryotic protein is a trimer of net charge -60, whereas the bacterial protein is a dimer of charge -22 (Fig. 3A). Despite these differences, both proteins generate almost identical positive $\phi(r)$ distributions in the DNA binding region.

Patterns of surface potentials have also provided a useful basis for interpreting biological and biochemical data and can point to residues that may play important func-

tional roles. For example, Ryu *et al.* (27) observed that a negative $\phi(r)$ site on an otherwise positive face of CD4 corresponded to a region implicated in cell fusion between HIV-infected cells and normal CD4-positive cells (Fig. 3C). MacDonald *et al.* (28), in analyzing their structure of NGF, noticed a positive groove at one end of the dimer. Six lysines line this groove, and their neutralization has a profound effect on the calculated $\phi(r)$ for this surface (Fig. 3D). Using site-directed mutagenesis (SDM), Ibanez *et al.* (29) were then able to show that these lysines are essential for the binding affinity of NGF to its "low-affinity" receptor.

The accuracy of the calculated $\phi(r)$'s (for example, Figs. 1 through 3) can be tested by SDM. One approach, pioneered by Fersht and co-workers (30), is to use SDM to modify a charge at a particular site on the protein surface and to measure shifts in pK_a, that is, the proton affinity, of acids and bases at other sites (K_a is the acid constant). The change in $\phi(r)$ calculated at these sites can then be related to the shifts by the simple relation $\Delta pK_a = \Delta\phi/2.3RT$ (R being the gas constant). Loewenthal *et al.* (31) reported extensive studies of charge-charge interactions on different proteins as a function of ionic strength and found that PB calculations done with the DelPhi program yielded results that were in impressive agreement with experiment.
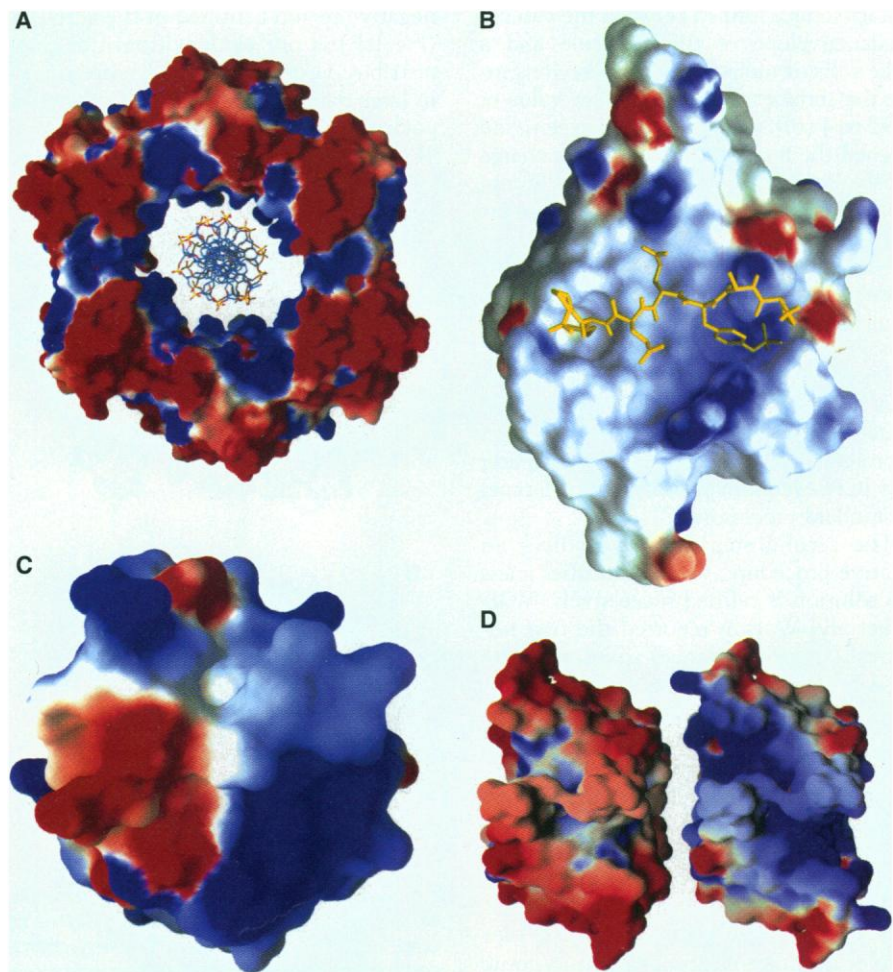
Fig. 3. Surface $\phi(r)$'s of various proteins. (**A**) The DNA binding beta subunit (processivity factor) from *E. coli* DNA polymerase III (74). A DNA molecule has been modeled into the center of the dimer where, despite a net negative charge of -22, the electrostatic potential is positive. (**B**) The Src SH2 domain (22), which binds a phosphotyrosine-containing peptide (shown in a bond representation). The phosphotyrosine binds in a distinctly positive pocket, while an isoleucine side chain from the peptide occupies a similar but neutral depression. (**C**) A view of CD4 (27) illustrating a negative patch on the mainly positive face of the protein that has been associated with cell fusion events. (**D**) Two views of the end of the NGF dimer (28) implicated in low-affinity receptor binding. On the left, the potential is that of the wild-type protein, whereas the potentials on the right were calculated with six lysine residues lining the groove treated as uncharged. The lysines in question are necessary for low-affinity receptor binding (29). Potentials are from DelPhi, with dielectrics as in Fig. 2B. The color code is as in Figs. 1 and 2, but the values used to determine the saturations varied; white is always equal to neutral. The ionic strength is zero in all cases except (A), where 0.1 M salt was assumed.

How Proteins Exploit Electrostatic Potentials

In addition to their role in molecular recognition, numerous examples exist where calculated $\phi(r)$'s of proteins have been implicated in different functional roles. A particularly striking effect is the enhancement of the diffusion-limited association constant of charged substrates (9, 32, 33).

The most detailed studies of association constants have been carried out on Cu,Zn superoxide dismutase (SOD), which, despite its net negative charge, generates a region of positive $\phi(r)$ near the active site (32). These $\phi(r)$'s are magnified in solution through the active-site focusing effects analogous to those for trypsin (9) (Fig. 2). Electrostatic focusing by narrow clefts appears to be a general phenomenon and may account, for example, for the production of large ion concentrations near the openings of transmembrane channels. Brownian dynamics simulations of the diffusion process in SOD have demonstrated that the focused $\phi(r)$ enhances the association rate of the negatively charged superoxide substrate (34, 35). The calculated rates are in excellent agreement with the experimental rate and its ionic strength dependence. Predictions of the effects of specific amino acid mutations on association rates (35) have been confirmed by recent SDM studies (36).

In addition to their effects on diffusion, $\phi(r)$'s also play an important role in the enhancement of catalytic rates (37), control by phosphorylation (38), and determination of redox potentials (39). A role for electrostatic surface potentials that has only recently been proposed for the bifunctional enzyme thymidylate synthase–dihydrofolate reductase is the channeling across the protein surface of a substrate between the two active sites (40).

Calculating pK_a's: pH Effects on Binding and Stability

The pK_a's of ionizable groups in macromolecules can be significantly different than those of the isolated groups in solution. Shifts in pK_a's between native and denatured states or between bound and free forms of a complex give rise to pH effects on macromolecular stability and on binding constants (41). For example, the acid denaturation of proteins appears largely as the result of a small number of amino acids whose pK_a's are shifted anomalously in the native protein (42, 43).

In proteins, pK_a's are typically calculated as pK_a shifts relative to the isolated amino acid. The source of the shifts has traditionally been attributed to interactions among ionizable groups on the macromolecule; for example, an acidic group will have its pK_a lowered through favorable interactions with basic groups. However, hydrogen bonding interactions with nonionizable groups and the degree of exposure to the bulk solvent have also been found to be important determinants of pK_a's (44). For example, an acidic group will have its pK_a increased if it is fully or partially removed from solvent, but the effect may be reversed by strong hydrogen bonding interactions with other groups. Thus, a full treatment of pH-dependent effects requires that the detailed environment of each ionizable group be taken into account. In addition to the need for structural detail, the problem of calculating pK_a's is further compounded by the fact that a protein with N ionizable residues has 2^N possible ionization states. Because a moderately sized protein may contain as many as 50 ionizable groups, methods have been developed to reduce the number of states that need to be considered.

Recent studies have addressed the combinatorial problem and, in addition, have used PB calculations to account for both desolvation effects and hydrogen bonding interactions (45). Applications to a few proteins have been reported, and the agreement with experimentally determined pK_a's has been good, with a few notable exceptions. A limitation on the accuracy of such calculations arises from uncertainties as to the nature of the conformational changes that accompany changes in the ionization states of different residues. Nevertheless, the available methods now allow a detailed study of the structural origins of pH effects on protein stability (43, 46) and substrate binding (47). Moreover, they can be used to generate structure-based predictions as to the contribution of specific ionizable residues to pH-dependent phenomena that can be tested with SDM.

The methodology developed primarily for the calculation of pK_a's in proteins has made it possible to solve a classical problem in physical organic chemistry. Dibasic and diacidic organic compounds such as succinic acid and 1,3-diamino propane exhibit two pK_a's that generally have been attributed to pK_a shifts in one group caused by its proximity to the charge on the other. Kirkwood and Westheimer (48) approached this problem more than 50 years ago by using classical electrostatics and treating the solute as a low-ϵ spherical cavity. The results were in qualitative agreement with experiment but depended on the detailed mapping of the solute charges onto a sphere. Quite recently, two groups have reinvestigated this problem using numerical solutions to the PB equation, and the results were in excellent agreement with experiment (49).

Salt Effects on Nucleic Acids

The large negative charge density generated by the phosphodiester backbone of nucleic acids results in a significant concentration of counterions in the vicinity of these macromolecules. For this reason, conformational changes and binding reactions involving DNA and RNA are strongly dependent on salt concentration (50). Salt effects on nucleic acids have been traditionally analyzed in terms of counterion condensation theory, which predicts that an essentially fixed concentration of counterions is found near the DNA, independent of bulk salt concentration (51). Manning (51) and Record and co-workers (52) have developed theoretical models that have been extremely successful in the interpretation of ligand binding equilibria and conformational transitions of nucleic acids, based on simplified representations of these molecules.

The availability of solutions to the nonlinear PBE (11, 53) and a general expression to obtain electrostatic free energies from the calculated $\phi(r)$'s (54) now makes it possible to make quantitative predictions of salt effects on the basis of 3D structures. The counterion concentration near nucleic acids is relatively insensitive to bulk salt concentration. Nevertheless, variations in this distribution near the surface of the molecule play a central role in determining salt effects on the conformational changes and binding reactions of nucleic acids. In applications to the problem of ligand binding to DNA, the dependence of the equilibrium constant on monovalent ion concentration was calculated for minor groove binding drugs (55) and for a number of proteins (56). In all cases, the calculated salt dependence of binding was in excellent agreement with experimental observation. Surprisingly, the major contribution was not the entropic release of counterions, which has been the standard view, but rather the changes in interaction of DNA with its ion atmosphere, which is a strong function of bulk ion concentration. Although studies of this type are still in their infancy, the results obtained so far indicate that it is now possible to obtain accurate predictions of nonspecific salt effects on the properties of highly charged polymers, even when large salt concentrations are involved.

Solvation Free Energies

Solvation phenomena can be described at the macroscopic level in terms of the difference in the reaction field energy of a charge distribution upon being transferred from one dielectric medium to another. The simplest problem of this type concerns the transfer free energy of an ion, which was treated by Born in 1920 as a uniformly

charged sphere (1). The vacuum-to-water hydration free energies of both anions and cations can be reproduced quite accurately with the Born model if a physically meaningful set of cavity radii are used (57). The remarkable success of the simple Born model has led to a resurgence in the use of continuum models to study solvation phenomena (58, 59). Electrostatic contributions to solvation free energies (ΔG^{solv}) with the PB method are in excellent agreement with those obtained from detailed microscopic solvent simulations (59, 60). Thus, classical electrostatics can reproduce the energetics of microscopic hydrogen bonding interactions of polar molecules with the aqueous phase.

In order to obtain values of ΔG^{solv} that can be compared with experimental values, both nonpolar and electrostatic contributions must be considered. Nonpolar contributions can also be treated at the macroscopic level through the use of surface tension concepts; that is, relations between free energy and surface area. The total free energy of transfer of a solute from the gas phase to water can be written as

$$\Delta G^{solv} = \Delta G^{np} + \Delta G^{es} \qquad (2)$$

where ΔG^{es} is the difference in electrostatic free energy of the solute in the two phases and ΔG^{np} corresponds to the free energy of inserting a hypothetical nonpolar solute of the same size and shape as the present solute into the solvent (61). It is frequently assumed, on the basis of earlier studies of alkane-water partition coefficients (62), that ΔG^{np} is proportional to accessible surface area (63) and is given by

$$\Delta G^{np} = \gamma^{vw} \Delta A^T + b \qquad (3)$$

where γ^{vw} is a constant that may be viewed as representing the vacuum-water microscopic surface tension, ΔA^T is the total accessible area of the solute, and b is a constant (note that the area is total area rather than just nonpolar area because all polar groups are assigned a charge of zero in the transfer step). The constants b (frequently assumed to be zero) and γ^{vw} are generally obtained by fitting the gas phase–to–water partition coefficients of linear alkanes (64) to a linear function of accessible surface area.

Atomic charges used in PB calculations of solvation phenomena are typically obtained from molecular mechanics force fields but can be treated as parameters as well (65). The results obtained so far suggest that PB calculations can be used on a solute described in terms of standard atomic radii and charges to obtain ΔG^{solv} values that agree with experiment for a large number of organic molecules. An alternative to using atomic charges extracted from force fields is to obtain the electronic distribution directly from quantum mechanics. Methods are now available that combine quantum mechanical calculations and continuum solvent models to yield solvation free energies that are in excellent agreement with experiment (66).

Effects of Solvation on Stability and Binding

The existence of complementary charged surfaces is a good indicator of association interfaces between different macromolecules. However, this does not necessarily imply a favorable electrostatic contribution to the free energy of association. Indeed, in many cases that have been studied, electrostatic interactions between groups of opposite charge actually oppose binding (67). The effect may be understood from the fact that the formation of, for example, an ion pair at an interface between two macromolecules involves the removal of the charged moieties from water. The desolvation costs associated with this process appear in general to be larger than the pairwise Coulombic interaction energy. The point was first made in a biological context by Parseghian (68), who argued that the removal of two oppositely charged ions from the aqueous phase that then form an ion pair in a lipid bilayer was costly in a free energy sense because the loss of favorable solvation interactions would not be compensated by Coulombic attraction. The validity of this argument has been subsequently verified by more detailed analysis (69).

An identical argument suggests that electrostatic interactions destabilize folded proteins even when there is a net Coulombic attraction between surface groups. Indeed, a study of the pH dependence of protein stability showed that ionizable groups destabilize proteins at all pH values (45). Recently, Hendsch and Tidor (70) found that salt bridges appear in general to destabilize proteins because of incomplete Coulombic compensation of desolvation effects.

The same type of argument appears to apply to hydrogen bonds as well. The electrostatic free energy loss associated with the removal of hydrogen bonding donor and acceptor groups from water is not generally compensated by the formation of a hydrogen bond in an interface or in the interior of a protein (71). If the anecdotal evidence available so far is verified, the rather global implication is that electrostatic interactions tend to favor the unfolded states of macromolecules and the unbound state of complexes. This would imply that the thermodynamic driving force for most processes in aqueous solution results from "nonpolar" interactions such as the hydrophobic effect and close packing. In this model, electrostatics in biological systems confer specific-

ity and play a role in the generation of unique structures (70, 72). In other words, once charged and polar groups have been removed from water, they must arrange to form ion pairs or hydrogen bonds so as to minimize the free energetic cost of their removal from water. A corollary of this argument is that the presence of polar groups in interfaces or in the interior of macromolecules has a destabilizing effect, reducing association constants and unfolding free energies.

Conclusions and Future Prospects

Continuum electrostatics as a tool for the analysis of molecular structure and function in solution has seen a major renaissance in recent years. Progress has been due in part to computational developments such as fast numerical solutions to the PB equation, fast algorithms to represent molecular surfaces, and new visualization techniques. However, equally important has been the development of methods to map molecular properties onto the language of continuum electrostatics and the recognition that many solvent effects can be treated accurately with a model that ignores the microscopic description of solvent molecules.

Graphical visualization of the electrostatic properties of macromolecular structures is having significant impact on the field of structural biology. Continuum electrostatics has also proved to be an extremely useful quantitative tool, allowing the accurate prediction of the magnitude of electrostatic effects. These developments offer the hope of a complete and accurate method to describe the properties of molecules in aqueous solution, although much remains to be done before this goal is realized. A major problem results from the fact that almost all applications of continuum methods have been to fixed structures. This is clearly adequate for many problems, but there are many other cases for which dynamical effects will have to be considered. The inclusion of continuum methods in dynamical studies, such as the direct incorporation of PB solutions into molecular mechanics force fields, has been attempted in a number of cases but remains a significant and important theoretical challenge (73).

Overall, the greatest impact of continuum methods results from the fact that they offer an intuitively simple yet physically complete model of molecules in solution. Fairly reliable predictions, both quantitative and qualitative, can be obtained with only moderate computational expense and are available to researchers on standard workstations. Equally important, general physical principles based on classical electrostatics are emerging that can be of con-

siderable value in the design and interpretation of experimental results. These developments have been made possible by the advent of fast computers and the application of sophisticated numerical methods, which have revived classical theory as a critical tool in the study of contemporary problems.

REFERENCES AND NOTES

1. M. Born, *Z. Phys.* **1**, 45 (1920).
2. J. G. Kirkwood, *J. Chem. Phys.* **7**, 911 (1939).
3. L. Onsager, *J. Am. Chem. Soc.* **58**, 1486 (1936).
4. Y. Vorobjev, H. Scheraga, B. Hitz, B. Honig, *J. Phys. Chem.* **98**, 10940 (1994).
5. F. M. Richards, *Annu. Rev. Biophys. Bioeng.* **6**, 151 (1977).
6. S. C. Harvey, *Proteins* **5**, 78 (1989); K. Sharp and B. Honig, *Annu. Rev. Biophys. Biophys. Chem.* **19**, 301 (1990).
7. G. Perrot *et al.*, *J. Comput. Chem.* **13**, 1 (1992); S. Sridharan, A. Nicholls, B. Honig, *Biophys. J.* **61**, A174 (1992); F. Eisenhaber and P. Argos, *J. Comput. Chem.* **14**, 1272 (1993).
8. J. Warwicker and H. C. Watson, *J. Mol. Biol.* **157**, 671 (1982).
9. I. Klapper, R. Hagstrom, R. Fine, K. Sharp, B. Honig, *Proteins* **1**, 47 (1986).
10. J. Warwicker, *J. Theor. Biol.* **121**, 199 (1986).
11. B. Jayaram, K. A. Sharp, B. Honig, *Biopolymers* **28**, 975 (1989).
12. A. Nicholls and B. Honig, *J. Comput. Chem.* **12**, 435 (1991).
13. M. E. Davis and J. A. McCammon, *ibid.* **10**, 386 (1989); M. Holst and F. Saied, *ibid.* **14**, 105 (1993).
14. R. Zauhar and R. J. Morgan, *J. Mol. Biol.* **186**, 815 (1985); A. A. Rashin, *J. Phys. Chem.* **94**, 725 (1990).
15. T. J. You and S. C. Harvey, *J. Comput. Chem.* **14**, 484 (1993).
16. M. K. Gilson, K. A. Sharp, B. H. Honig, *ibid.* **9**, 327 (1988).
17. A. Nicholls, K. A. Sharp, H. Honig, *Proteins* **11**, 281 (1991).
18. J. L. Sussman *et al.*, *Science* **253**, 872 (1991).
19. W. Bode and P. Schwager, *J. Mol. Biol.* **98**, 693 (1975).
20. See, for example, J. Guenot, R. Fletterick, P. Kollman, *Protein Sci.* **3**, 1276 (1994).
21. J. Kuriyan and M. O'Donnell, *J. Mol. Biol.* **234**, 915 (1993).
22. G. Waksman, S. E. Shoelson, N. Pant, D. Cowburn, J. Kuriyan, *Cell* **72**, 779 (1993).
23. J. Abrahams, A. Leslie, R. Lutter, J. Walker, *Nature* **370**, 621 (1994).
24. D. L. Scott, A. M. Mandel, P. B. Sigler, B. Honig, *Biophys. J.* **67**, 493 (1994).
25. M. Ryden *et al.*, *EMBO J.* (1994).
26. T. S. R. Krishna, X.-P. Kong, S. Gary, P. Burgers, J. Kuriyan, *Cell* **79**, 1233 (1994).
27. S. Ryu *et al.*, *Nature* **348**, 419 (1990).
28. N. Q. McDonald *et al.*, *ibid.* **354**, 411 (1991).
29. C. F. Ibanez *et al.*, *Cell* **69**, 329 (1992).
30. P. G. Thomas, A. G. Russell, A. J. Fersht, *Nature* **318**, 375 (1985).
31. R. Loewenthal, J. Sancho, T. Reinikainen, A. R. Fersht, *J. Mol. Biol.* **232**, 574 (1993).
32. E. D. Getzoff *et al.*, *Nature* **306**, 287 (1983).
33. W. Koppenol and E. Margoliash, *J. Biol. Chem.* **257**, 4426 (1982); D. Ripoll, C. Faerman, P. Axelsen, I. Sillman, J. Sussman, *Proc. Natl. Acad. Sci. U.S.A.* **90**, 5128 (1993).
34. S. A. Allison, R. Bacquet, J. A. McCammon, *Biopolymers* **27**, 251 (1988).
35. K. Sharp, R. Fine, B. Honig, *Science* **236**, 1460 (1987); J. Sines, S. Allison, J. McCammon, *Biochemistry* **29**, 9403 (1990).
36. E. D. Getzoff *et al.*, *Nature* **358**, 347 (1992).
37. A. Warshel, *Biochemistry* **20**, 3167 (1981); _____, G. Naray-Szabo, F. Sussman, J. Hwang, *ibid.* **28**, 3629 (1989); K. Soman, A.-S. Yang, B. Honig, R. Fletterick, *ibid.*, p. 9918.
38. J. H. Hurley, A. M. Dean, J. L. Sohl, D. E. Koshland Jr., R. M. Stroud, *Science* **249**, 1012 (1990); L. Johnson and D. Barford, *Protein Sci.* **3**, 1726 (1994).
39. A. K. Churg and A. Warshel, *Biochemistry* **25**, 1675 (1986); M. R. Gunner and B. Honig, *Proc. Natl. Acad. Sci. U.S.A.* **88**, 9151 (1991).
40. D. Knighton *et al.*, *Nature Struct. Biol.* **1**, 186 (1994).
41. C. Tanford and R. Roxby, *Biochemistry* **11**, 2192 (1972).
42. C. N. Pace, D. V. Laurents, J. A. Thomson, *ibid.* **29**, 2564 (1990); C.-Q. Hu, J. M. Sturtevant, J. A. Thomson, R. E. Erickson, C. N. Pace, *ibid.* **31**, 4876 (1992).
43. A.-S. Yang and B. Honig, *J. Mol. Biol.* **231**, 459 (1993).
44. A. Warshel and S. Russell, *Q. Rev. Biophys.* **17**, 283 (1984).
45. D. Bashford and M. Karplus, *Biochemistry* **29**, 10219 (1990); P. Beroza, D. R. Fredkin, M. Y. Okamura, G. Feher, *Proc. Natl. Acad. Sci. U.S.A.* **88**, 5804 (1991); A.-S. Yang, M. R. Gunner, R. Sampogna, K. Sharp, B. Honig, *Proteins* **15**, 252 (1993); M. K. Gilson, *ibid.*, p. 266.
46. A.-S. Yang and B. Honig, *J. Mol. Biol.* **237**, 602 (1994).
47. A. MacKerell, M. S. Somner, M. Karplus, *ibid.* **247**, 774 (1995).
48. J. Kirkwood and F. Westheimer, *J. Chem. Phys.* **6**, 506 (1938).
49. E. Rajasekran, B. Jayaram, B. Honig, *J. Am. Chem. Soc.* **116**, 8238 (1994); M. Potter, M. Gilson, J. McCammon, *ibid.*, p. 10298.
50. P. L. de Haseth, T. M. Lohman, M. T. Record, *Biochemistry* **16**, 4783 (1977).
51. G. S. Manning, *Q. Rev. Biophys.* **11**, 179 (1978).
52. M. T. Record, C. F. Anderson, T. M. Lohman, *ibid.*, p. 103; M. T. Record, M. Olmsted, C. F. Anderson, in *Theoretical Chemistry and Molecular Biophysics*, D. L. Beveridge and R. Lavery, Eds. (Adenine, Schenectady, NY, 1990), vol. 1, pp. 285-308; C. A. Anderson and M. T. Record, *J. Phys. Chem.* **97**, 7116 (1993).
53. H. Oberoi and N. Allewell, *Biophys. J.* **65**, 48 (1993); M. Holst, R. Kozack, F. Saied, S. Subramaniam, *Proteins* **18**, 231 (1994).
54. K. A. Sharp and B. Honig, *J. Phys. Chem.* **94**, 7684 (1990); K. Sharp, R. A. Friedman, V. Misra, J. Hecht, B. Honig, *Biopolymers*, in press.
55. V. K. Misra, K. A. Sharp, R. A. Friedman, B. Honig, *J. Mol. Biol.* **238**, 245 (1994).
56. M. Zacharias, B. A. Luty, M. E. Davis, J. A. McCammon, *Biophys. J.* **63**, 1280 (1992); V. K. Misra, J. L. Hecht, K. A. Sharp, R. A. Friedman, B. Honig, *J. Mol. Biol.* **238**, 264 (1994).
57. A. A. Rashin and B. Honig, *J. Phys. Chem.* **89**, 5588 (1985).
58. A. A. Rashin and K. Namboodiri, *ibid.* **91**, 6003 (1987); M. K. Gilson and B. Honig, *Proteins Struct. Funct. Genet.* **4**, 7 (1988); A. Rashin and M. Bukatin, *Biophys. Chem.* **51**, 167 (1994).
59. V. Mohan, M. E. Davis, J. A. McCammon, B. M. Pettitt, *J. Phys. Chem.* **96**, 6428 (1992).
60. A. Jean-Charles *et al.*, *J. Am. Chem. Soc.* **113**, 1454 (1991).
61. K. Sharp, A. Jean-Charles, B. Honig, *J. Phys. Chem.* **96**, 3822 (1992).
62. R. B. Hermann, *ibid.* **76**, 2754 (1972).
63. B. Lee and F. M. Richards, *J. Mol. Biol.* **55**, 379 (1971).
64. A. Ben-Naim and Y. Marcus, *J. Chem. Phys.* **81**, 2016 (1984).
65. D. Sitkoff, K. A. Sharp, B. Honig, *J. Phys. Chem.* **98**, 1978 (1994); T. Simonson and A. Brünger, *ibid.*, p. 4683.
66. S. Miertus, E. Scrocco, J. Tomasi, *J. Chem. Phys.* **55**, 117 (1981); C. J. Cramer and D. G. Truhlar, *J. Comput. Aided Mol. Des.* **6**, 629 (1992); V. Luzhkov and A. Warshel, *J. Comput. Chem.* **13**, 199 (1992); A. Rashin, M. Bukatin, J. Andzelm, A. Hagler, *Biophys. Chem.* **51**, 375 (1994); J. Chen, L. Noodleman, D. Case, D. Bashford, *J. Phys. Chem.* **98**, 11059 (1994); D. Tannor *et al.*, *J. Am. Chem. Soc.* **116**, 11875 (1994).
67. See, for example, J. Novotny and K. Sharp, *Prog. Biophys. Mol. Biol.* **58**, 203 (1992).
68. V. Parseghian, *Nature* **221**, 884 (1969).
69. B. Honig and W. L. Hubbell, *Proc. Natl. Acad. Sci. U.S.A.* **81**, 5412 (1984).
70. Z. Hendsch and B. Tidor, *Protein Sci.* **3**, 211 (1994).
71. M. Gilson and B. Honig, *Proc. Natl. Acad. Sci. U.S.A.* **86**, 1524 (1989); A. Ben-Naim, *J. Phys. Chem.* **95**, 1437 (1991); A.-S. Yang, K. Sharp, B. Honig, *J. Mol. Biol.* **227**, 889 (1992).
72. A. Fersht, *Trends Biochem Sci.* **9**, 145 (1984); A.-S. Yang and B. Honig, *Adv. Protein Chem.* **46**, 27 (1995).
73. M. Gilson and B. Honig, *J. Comput. Aided Mol. Des.* **5**, 5 (1991); K. A. Sharp, *J. Comput. Chem.* **12**, 454 (1991); R. Zauhar, *ibid.*, p. 575; M. K. Gilson, M. E. Davis, B. A. Luty, A. McCammon, *J. Phys. Chem.* **97**, 3591 (1993); R. Abagyan and M. Totrov, *J. Mol. Biol.* **235**, 983 (1994).
74. X.-P. Kong, R. Onrust, M. O'Donnell, J. Kuriyan, *Cell* **63**, 425 (1992).